Further investigation of the relativistic symmetry by similarity renormalization group

Dong-Peng Li, Shou-Wan Chen, Jian-You Guo[1, *]

[1] *School of Physics and Material Science, Anhui University, Hefei 230039, People's Republic of China*

Following a recent rapid communications[Phys.Rev.C85,021302(R) (2012)], we present more details on the investigation of the relativistic symmetry by use of the similarity renormalization group. By comparing the contributions of the different components in the diagonal Dirac Hamiltonian to the pseudospin splitting, we have found that two components of the dynamical term make similar influence on the pseudospin symmetry. The same case also appears in the spin-orbit interactions. Further, we have checked the influences of every term on the pseudospin splitting and their correlations with the potential parameters for all the available pseudospin partners. The result shows that the spin-orbit interactions always play a role in favor of the pseudospin symmetry, and whether the pseudospin symmetry is improved or destroyed by the dynamical term relating the shape of the potential as well as the quantum numbers of the state. The cause why the pseudospin symmetry becomes better for the levels closer to the continuum is disclosed.

PACS numbers: 21.10.Hw,21.10.Pc,03.65.Pm,05.10.Cc

I. INTRODUCTION

More than 40 years ago, a quasidegeneracy was observed in heavy nuclei between two single-particle states with the quantum numbers $(n-1, l+2, j=l+3/2)$ and $(n, l, j=l+1/2)$. In analogy with the well known spin-symmetry (SS) breaking for the spin doublets $(n, l, j=l\pm 1/2)$, which is one of the most important concepts for understanding the traditional magic number in atomic nuclei [1, 2], the pseudospin symmetry (PSS) was proposed by defining the pseudospin doublets ($\tilde{n}=n-1$, $\tilde{l}=l+1$, $j=\tilde{l}\pm 1/2$) [3, 4]. The introduction of the PSS concept has explained numerous phenomena in nuclear structure including deformation [5], superdeformation [6], identical bands [7], and magnetic moment [8]. Especially for the magic number change in exotic nuclei, the spin and pseudospin symmetries are pointed out to play important roles. For instance, the $N=28$ shell closure disappears due to the quenching of the spin-orbit splitting for the $\nu 1f$ spin doublets [9–12], and the $Z=64$ sub-shell closure is closely related to the restoration of PSS for the $\pi 2\tilde{p}$ and $\pi 1\tilde{f}$ pseudospin doublets [13–15]. Because of these successes, there have been comprehensive efforts to understand the origin of this symmetry as well as its breaking mechanism. Based on the single-particle Hamiltonian of the oscillator shell model, Bahri et al. indicated that the origin of PSS is connected with a special ratio in the strength of the spin-orbit and orbit-orbit interactions, and the ratio can be partly explained by the relativistic mean field theory [16]. Blokhin et al. introduced a helicity unitary transformation which can map a normal state (l, s) to a pseudo state $(\tilde{l}, \tilde{s})$ [17]. A substantial progress was achieved in Ref. [18], where the relativistic feature of PSS was recognized. The pseudo-orbital angular momentum $\tilde{l}$ is nothing but the orbital angular momentum of the lower component of the Dirac spinor, and the equality in magnitude but difference in sign of the scalar potential S and vector potential V was suggested as the exact PSS limit. In a more general condition, the exact PSS is satisfied in the Dirac equation when the sum of the scalar S and vector V potentials is equal to a constant [19]. Moreover, the PSS in real nuclei was shown in connection with the competition between the pseudocentrifugal barrier and the pseudospin-orbital potential [20, 21]. Even with these excellent work mentioned above, there is still much attention on the cause of splitting for the reason that the exact PSS cannot be met in real nuclei. In Refs. [22–24], it was pointed out that the observed pseudospin splitting arises from a cancelation of the several energy components, and the PSS in nuclei has a dynamical character. A similar conclusion was reached in Refs. [25, 26]. In addition, it was noted that, unlike the spin symmetry, the pseudospin breaking cannot be treated as a perturbation of the pseudospin-symmetric Hamiltonian[27]. The nonperturbation nature of PSS has also been mentioned in Ref. [28]. Further, the supersymmetric description of PSS was presented for the spherical nuclei and axially deformed nuclei [29–31]. In a very recent paper [32], supersymmetric quantum mechanics and similarity renormalization group (SRG) are used as the critical tools for understanding the origin of PSS and its breaking mechanism, and the cause why the PSS becomes better for the levels closer to the continuum is discussed in a quantitative way at the nonrelativistic limit. This symmetry is also checked in the resonant states [33, 34] with similar features to bound states indicated

*E-mail:jianyou@ahu.edu.cn

in Ref. [35].

Regardless of these pioneering studies, the origin of PSS has not been fully understood in the relativistic framework. Recently, we have examined the PSS by use of the similarity renormalization group and shown explicitly the relativistic origin of this symmetry [36]. We have also studied the relativistic effect of this symmetry [37]. However, we have not researched the dependence of PSS on the shape of the potential and the quantum numbers of the states by using this Hamiltonian. Although the correlation of the energy splitting of pseudospin partners with the nuclear potential parameters has been investigated by solving the Dirac equation with Woods-Saxon scalar and vector radial potentials [22, 23], we do not know the relationship between the splitting of every component and the shape of the potential, which is particularly important to reveal the origin of PSS. In this paper, we explore the dependence of the PSS on the shape of the potential and the quantum numbers of the states by using this Hamiltonian obtained in Ref. [36] in order to disclose the influence of every component, especially those relating the dynamical effect and the spin-orbit interactions.

II. FORMALISM

For simplicity, we sketch our formalism with the following Dirac Hamiltonian:

$$H_D = \begin{pmatrix} M+\Sigma(r) & -\frac{d}{dr}+\frac{\kappa}{r} \\ \frac{d}{dr}+\frac{\kappa}{r} & -M+\Delta(r) \end{pmatrix}, \tag{1}$$

where $\Sigma(r) = V(r) + S(r)$ and $\Delta(r) = V(r) - S(r)$ denote the combinations of the scalar potential $S(r)$ and the vector potential $V(r)$ and κ is defined as $\kappa = (l-j)(2j+1)$. To extract the different components from H_D, the SRG is used to transform the Dirac Hamiltonian into a block-diagonal form. The details can be referred to the literature [36]. The diagonal Dirac Hamiltonian is written as

$$H_D = \begin{pmatrix} H_P + M & 0 \\ 0 & -H_P^C - M \end{pmatrix}, \tag{2}$$

where

$$\begin{aligned} H_P \;=\; & \Sigma(r) + \frac{p^2}{2M} - \frac{1}{2M^2}\left(Sp^2 - S'\frac{d}{dr}\right) - \frac{\kappa}{r}\frac{\Delta'}{4M^2} + \frac{\Sigma''}{8M^2} \\ & + \frac{S}{2M^3}\left(Sp^2 - 2S'\frac{d}{dr}\right) + \frac{\kappa}{r}\frac{S\Delta'}{2M^3} - \frac{\Sigma'^2 - 2\Sigma'\Delta' + 4S\Sigma''}{16M^3} - \frac{p^4}{8M^3} + O\left(\frac{1}{M^4}\right) \end{aligned} \tag{3}$$

is an operator describing Dirac particle with $p^2 = -\frac{d^2}{dr^2} + \frac{\kappa(\kappa+1)}{r^2}$, and H_P^C is the charge-conjugation of H_P [24, 38]. The charge-conjugation operator is given by $C = i\gamma^2 K$, where K is the complex conjugation operator [39]. The primes and the double primes in H_P respectively denote first- and second-order derivatives with respect to r. From Eq.(3), we see that the present transformation avoids all the drawbacks in the usual decoupling [22, 23], and H_P holds the form of Schrödinger-like operator.

III. THE NUMERICAL CALCULATIONS AND DISCUSSIONS

With the formalism represented in the previous section, we explore the origin of PSS by use of H_P. To convince the reliability of the present calculations, we first check the convergence of the expansion in Eq. (3). For convenience in the numerical computations, a Woods-Saxon type potential is adopted for $\Sigma(r)$ and $\Delta(r)$, i.e., $\Sigma(r) = \Sigma_0 f(a_\Sigma, r_\Sigma, r)$ and $\Delta(r) = \Delta_0 f(a_\Delta, r_\Delta, r)$ with

$$f(a, R, r) = \frac{1}{1 + \exp\left(\frac{r-R}{a}\right)}. \tag{4}$$

which is realistic enough to be applied to nuclei although it is not a full self-consistent relativistic potential derived from meson fields [23]. Using this potential for $\Sigma(r)$ and $\Delta(r)$, there are six parameters, i.e., the central depths, Σ_0 and Δ_0, two radii, and two diffuseness parameters. Following Refs. [23], the same radius R and surface diffuseness a are set for the both potentials $\Sigma(r)$ and $\Delta(r)$, and Σ_0, Δ_0, a, and R are determined by fitting the neutron spectra of ^{208}Pb with the fitted results: $\Sigma_0 = -66$ MeV, $\Delta_0 = 650$ MeV, $a = 0.6$ fm, and $R = 7$ fm. With the values for

TABLE I: The energy spectra of H_p for all the available bound states. The second column indicates that H_p is approximated to the nonrelativistic limit. The third and fourth columns indicate that H_p is approximated to the orders $1/M^2$ and $1/M^3$, respectively. For comparisons, the exact relativistic spectra are displayed in the fifth column.

i	Non	$1/M^2$(MeV)	$1/M^3$(MeV)	Exa(MeV)
$1s_{1/2}$	-61.123	-59.826	-59.408	-59.226
$2s_{1/2}$	-48.353	-43.689	-42.221	-41.609
$3s_{1/2}$	-30.377	-21.630	-19.118	-18.371
$1p_{3/2}$	-56.332	-53.843	-53.088	-52.782
$2p_{3/2}$	-40.463	-34.018	-32.104	-31.416
$3p_{3/2}$	-20.738	-10.783	-8.259	-7.706
$1p_{1/2}$	-56.332	-53.636	-52.723	-52.282
$2p_{1/2}$	-40.463	-33.608	-31.446	-30.625
$3p_{1/2}$	-20.738	-10.289	-7.599	-7.012
$1d_{5/2}$	-50.534	-46.710	-45.631	-45.252
$2d_{5/2}$	-31.981	-23.908	-21.675	-21.012
$1d_{3/2}$	-50.534	-46.194	-44.738	-44.071
$2d_{3/2}$	-31.981	-23.088	-20.423	-19.585
$1f_{7/2}$	-43.842	-38.626	-37.282	-36.898
$2f_{7/2}$	-23.031	-13.667	-11.312	-10.771
$1f_{5/2}$	-43.842	-37.651	-35.626	-34.790
$2f_{5/2}$	-23.031	-12.389	-9.483	-8.788
$1g_{9/2}$	-36.346	-29.767	-28.256	-27.936
$2g_{9/2}$	-13.770	-3.770	-1.636	-1.304
$1g_{7/2}$	-36.346	-28.183	-25.621	-24.714
$1h_{11/2}$	-28.128	-20.307	-18.757	-18.559
$1h_{9/2}$	-28.128	-17.976	-14.982	-14.128
$1i_{13/2}$	-19.263	-10.429	-8.995	-8.955
$1i_{11/2}$	-19.263	-7.259	-4.040	-3.371

the parameters, the energy spectra of H_P are obtained and listed in Table I in comparisons with the solutions of the original Dirac equation. From Table I, it can be seen that the deviations between the nonrelativistic limit (the second column) and the exact relativistic case (the fifth column) are very large, i.e., the relativistic effect is apparent in the present system. With the increasing perturbation order, the calculated result is closer to the exact relativistic one. When H_P is approximated to the order $1/M^3$, the calculated spectra are considerably agreeable with those from the exact relativistic calculations. These indicate that the convergence of the present expansion is satisfactory, and it is reasonable enough to probe the PSS hidden in Dirac Hamiltonian in terms of the operator H_P.

For analyzing the PSS, we decompose H_P into the eight components: $\Sigma(r) + \frac{p^2}{2M}$, $-\frac{1}{2M^2}\left(Sp^2 - S'\frac{d}{dr}\right)$, $\frac{S}{2M^3}\left(Sp^2 - 2S'\frac{d}{dr}\right)$, $-\frac{\kappa}{r}\frac{\Delta'}{4M^2}$, $\frac{\kappa}{r}\frac{S\Delta'}{2M^3}$, $\frac{\Sigma''}{8M^2}$, $-\frac{\Sigma'^2 - 2\Sigma'\Delta' + 4S\Sigma''}{16M^3}$, $-\frac{p^4}{8M^3}$, which are respectively labeled as $O_1, O_2, \ldots, O_8$. O_1 corresponds to the operator describing Dirac particle in the nonrelativistic limit. O_2 and O_3 are related to the dynamical effect. The spin-orbit interactions are reflected in the O_4 and O_5. In this decomposition $O_i (i = 1, 2, \ldots, 8)$ is Hermitian. Hence, it is easy to calculate the contribution of each component to the pseudospin splitting, which is helpful to disclose the origin of PSS. The contribution of O_i to the level E_k is calculated by the formula $\langle k| O_i |k\rangle = \int \psi_k^* O_i \psi_k d^3\vec{r}$, where ψ_k is a eigenvector of the k-state.

To clarify whether the quality of PSS originates mainly from the competition of the dynamical effect and the spin-orbit interactions, we compare the contributions of the dynamical components (O_2 and O_3) and the spin-orbit interactions (O_4 and O_5) to the energy splitting of pseudospin partner, and their correlations with the shape of potential and the quantum numbers of the state.

In Fig.1, we show the variation of the pseudospin energy splitting with the surface diffuseness a for the doublets $(3s_{1/2}, 2d_{3/2})$ and $(3p_{3/2}, 2f_{5/2})$, where the "dynam1" and "dynam2" present respectively the contributions of O_2 and O_3 to the energy splitting, and the "spin-orb1" and "spin-orb2" present respectively the contributions of O_4 and O_5 to the energy splitting. For guiding eyes, the total energy splitting is plotted as "total". The same labels are adopted in the following figures 2 and 3. From Fig.1, we can see that the pseudospin splitting caused by the component O_i $(i = 2, 3, 4, 5)$ is insensitive to a. The sensitivity of total energy splitting to a origins mainly from the contribution of the nonrelativistic part, which will be seen in the latter discussions. Over the range of a under consideration, these components relating the spin-orbit interactions always play a role in favor of the PSS, while the dynamical effect depends on the particular pseudospin doublet we are considering. For the doublet $(3s_{1/2}, 2d_{3/2})$, the pseudospin splitting is added by the contributions of the dynamical components, while for the doublet $(3p_{3/2}, 2f_{5/2})$, the pseudospin splitting is reduced by the contributions of the dynamical components. The same case also appears

in the energy splitting varying with the depth of potential well, which is plotted in Fig.2. Over the range of Σ_0 under consideration, the contributions of O_4 and O_5 to the energy splitting are negative, i.e., improve the PSS, while the contributions of O_2 and O_3 to the energy splitting are positive for the $(3s_{1/2}, 2d_{3/2})$, and negative for the $(3p_{3/2}, 2f_{5/2})$. The pseudospin energy splitting varying with the radius R is depicted in Fig.3. Similar to the previous two figures, the PSS is improved by the spin-orbit interactions for all the pseudospin partners considered here. But for the dynamical components, which contribute the pseudospin splitting evolving from a negative value to a positive value and inverting the sign of the energy splitting with the increasing of R. The trend of total energy splitting with R is consistent with that caused by the dynamical components. Especially for the $(3p_{3/2}, 2f_{5/2})$, the dynamical effect is sensitive to R. Whether the PSS is improved or destroyed by the dynamical components depends on the shape of potential.

From Figs.1-3, we have noticed that the contribution of O_2 to the pseudospin splitting is similar to that of O_3 except for the extent of splitting. When a splitting value caused by O_2 is negative, that by O_3 is also negative. With the change of the potential parameters, the variation of the splitting caused by O_2 is consistent with that by O_3, even the position of the splitting appearing inversion is same. The similar case also appears in the spin-orbit interactions (O_4 and O_5). Accordingly, to compare the contributions of these terms with different physical effect to the pseudospin splitting, we combine O_2 and O_3 as a dynamic term, and O_4 and O_5 as a spin-orbit coupling term. As the influences of O_6, O_7, and O_8 on the PSS are weak, we combine them as an other term. With these combinations, we compare the dependence of the contribution of every term to the pseudospin splitting on the shape of potential and the quantum numbers of the state for all the available pseudospin partners.

In Figs.4-6, we display the variation of the pseudospin energy splitting with the surface diffuseness a for the $(2p_{3/2}, 1f_{5/2})$, $(2d_{5/2}, 1g_{7/2})$, $(3s_{1/2}, 2d_{3/2})$, $(3p_{3/2}, 2f_{5/2})$, $(2f_{7/2}, 1h_{9/2})$, and $(2g_{9/2}, 1i_{11/2})$. The relativistic and nonrelativistic pseudospin splittings are sensitive to a. The trend of total energy splitting with a is similar to the nonrelativistic case. The contributions from the other parts in H_P almost do not alter with a. The variation of total energy splitting with a origins mainly from the nonrelativistic part. Nevertheless, the relativistic PSS is significantly improved, which comes mainly from the spin-orbit interactions and the dynamical effect. The improvement from the spin-orbit interactions increases with the increasing orbital angular momentum for the states with the same radial quantum number. Different from the spin-orbit interactions, the dynamical term destroys PSS for the deeply bound states $(2p_{3/2}, 1f_{5/2})$, $(2d_{5/2}, 1g_{7/2})$, $(3s_{1/2}, 2d_{3/2})$, and $(2f_{7/2}, 1h_{9/2})$, while improves PSS for the loosely bound states $(3p_{3/2}, 2f_{5/2})$ and $(2g_{9/2}, 1i_{11/2})$. The contributions of O_6, O_7, and O_8 to the pseudospin splitting are negligible.

The pseudospin energy splitting varying with the depth of potential is exhibited in Figs.7-9 for these partners shown in Figs.4-6. The potential depth Σ_0 almost does not affect the splitting contributed by the nonrelativistic part regardless of the splitting is serious. The evolution of pseudospin energy splitting with Σ_0 is mostly dominated by the spin-orbit interactions and the dynamical effect. Over the range of Σ_0 here, the improvement from the spin-orbit interactions increases with the increasing orbital angular momentum for the states with the same radial quantum number, which is similar to the case with a. Whether the PSS is improved or destroyed by the dynamical term relating the particular pseudospin doublet. For the pseudospin partners $(2p_{3/2}, 1f_{5/2})$, $(2d_{5/2}, 1g_{7/2})$, $(3s_{1/2}, 2d_{3/2})$, and $(2f_{7/2}, 1h_{9/2})$, the contribution of the dynamic term enlarges the pseudospin energy splitting. However for the $(3p_{3/2}, 2f_{5/2})$ and $(2g_{9/2}, 1i_{11/2})$, the contribution of the dynamical term reduces the pseudospin energy splitting, and the dynamical effect becomes an improvement to the PSS. The improvement increases as the potential depth becomes shallow. Compared with the spin-orbit interactions, the dynamic effect is more sensitive to Σ_0. Especially for the loosely bound states $(3p_{3/2}, 2f_{5/2})$ and $(2g_{9/2}, 1i_{11/2})$, the PSS improved with the gradually shallow potential well originates mainly from the dynamic effect.

Besides the a and Σ_0, the relationship of the pseudospin splitting and the radius R is more interesting. In Figs.10-12, we show the pseudospin energy splitting varying with R for all the available pseudospin partners. The nonrelativistic energy splitting decreases with the increasing of R, which is opposite with total energy splitting with a little exception (e.g., $(2p_{3/2}, 1f_{5/2})$). The increasing of total energy splitting with R arises from the contributions of the dynamical term and the spin-orbit interactions. Similar to the preceding case, the spin-orbit interactions always improve the PSS, but the improvement becomes weaker with the increasing of R. For the pseudospin partners $(2p_{3/2}, 1f_{5/2})$ and $(2d_{5/2}, 1g_{7/2})$, the dynamical effect is insensitive to R, and the variation of total energy splitting with R comes mainly from the the spin-orbit interactions. However for the other parters, the dynamic effect improves the PSS when R is small. With the increasing of R, the pseudospin splitting coming from the dynamic effect appears inversion, from an improvement to a breaking. Together, they create a variation of total energy splitting with R. But the sensitivity to R is different. For example the $(3p_{3/2}, 2f_{5/2})$ partner, the variation of total energy splitting with R origins mainly from the dynamic effect, the splitting from the spin-orbit interactions is almost independent of R.

Throughout Figs.4-12, the spin-orbit interactions and the dynamical effect play the key roles in influencing the PSS. Their contributions to the pseudospin energy splitting are correlated with the shape of the potential and the quantum numbers of the state. Compared with the spin-orbit interactions, the dependence of the dynamical effect on the shape of potential is more sensitive. Over the range of the potential parameters considered here, the spin-orbit interactions always play a role in improving the PSS. The improvement of the spin-orbit interactions to the PSS increases for these

levels closer to the continuum. However for the dynamical effect, it relates the shape of the potential as well as the quantum numbers of the state. For the deeply bound levels, the contribution of the dynamical term is a breaking of the PSS, while for the levels close to the continuum, the contribution of dynamical term becomes an improvement to the PSS. These have explained the reason why the levels are closer to the continuum, the PSS is better. In short, the quality of PSS is related to the shape of the potential and the quantum numbers of the state as well as the relativistic effect.

IV. SUMMARY

In summary, by using the Hamiltonian obtained from the usual Dirac Hamiltonian by the similarity renormalization group, we have researched in details the origin of the relativistic symmetry in nuclei. By comparing the contribution of the different components in the Dirac Hamiltonian H_P to the pseudospin energy splitting, and their relation to the shape of potential, it is found that two dynamic components make similar effect on the PSS. The same case also appears in the spin-orbit interactions. Further, we have checked the contribution of every term in the Hamiltonian H_P to the pseudospin splitting, and their correlations with the potential parameters for all the available pseudospin partners. The results show that the spin-orbit interactions and the dynamical effect play the major role in influencing the PSS. Their contributions to the pseudospin energy splitting are correlated with the shape of the potential and the quantum numbers of the state. Compared with the spin-orbit interactions, the dependence of the dynamical effect on the shape of potential is more sensitive. Over the range of the potential parameters considered here, the spin-orbit interactions always improves the PSS. For these levels closer to the continuum, the improvement of the spin-orbit interactions to the PSS is more obvious. However for the dynamical effect, whether the PSS is improved or destroyed by the dynamical term relating the shape of potential and the quantum numbers of the state. For the deeply bound levels, the contribution of the dynamical term to the pseudospin splitting is against that of the spin-obit interactions, the quality of PSS originates mainly from the competition of the dynamical effects and the spin-orbit interactions. However for the levels close to the continuum, the contribution of the dynamical term reduces the pseudospin splitting just like the spin-orbit interactions. These have explained the reason why the levels are closer to the continuum, the PSS is better. The quality of PSS is related to the shape of the potential and the quantum numbers of the state as well as the relativistic effect.

This work was partly supported by the National Natural Science Foundation of China under Grants No. 10675001, No. 11175001, and No. 11205004; the Program for New Century Excellent Talents in University of China under Grant No. NCET-05-0558; the Excellent Talents Cultivation Foundation of Anhui Province under Grant No. 2007Z018; the Natural Science Foundation of Anhui Province under Grant No. 11040606M07; the Education Committee Foundation of Anhui Province under Grant No. KJ2009A129; and the 211 Project of Anhui University.

[1] O. Haxel, J. H. D. Jensen, and H. E. Suess, Phys. Rev. **75**, 1766 (1949).
[2] M. Goeppert-Mayer, Phys. Rev. **75**, 1969 (1949).
[3] K. T. Hecht and A. Adler, Nucl. Phys. **A 137**, 129 (1969).
[4] A. Arima, M. Harvey, and K. Shimizu, Phys. Lett. **30 B**, 517 (1969).
[5] A. Bohr, I. Hamamoto, and B. R. Mottelson, Phys. Scr. **26**, 267 (1982).
[6] J. Dudek, W. Nazarewicz, Z. Szymanski, and G. A. Leander, Phys. Rev. Lett. **59**, 1405 (1987).
[7] W. Nazarewicz, P. J. Twin, P. Fallon, and J. D. Garrett, Phys. Rev. Lett. **64**, 1654 (1990).
[8] D. Troltenier, W. Nazarewicz, Z. Szymanski, and J. P. Draayer, Nucl. Phys. **A567**, 591 (1994).
[9] L. Gaudefroy, O. Sorlin, and D. Beaumel et al. Phys. Rev. Lett. **97**, 092501 (2006).
[10] B. Bastin, S. Grévy1, and D. Sohler et al. Phys. Rev. Lett. **99**, 022503 (2007).
[11] D. Tarpanov, H. Liang, N. V. Giai, and C. Stoyanov, Phys. Rev. **C 77**, 054316 (2008).
[12] M. Moreno-Torres, M. Grasso, H. Z. Liang, V. De Donno, M. Anguiano, and N. Van Giai, Phys. Rev. **C 81**, 064327 (2010).
[13] Y. Nagai, J. Styczen, and M. Piiparinen et al. Phys. Rev. Lett. **47**, 1259 (1981).
[14] W. H. Long, H. Sagawa, N. V. Giai, and J. Meng, Phys. Rev. **C 76**, 034314 (2007).
[15] W. H. Long, T Nakatsukasa, H. Sagawa, J. Meng, H. Nakada, and Y. Zhang, Phys. Lett. **B 680**, 428 (2009).
[16] C. Bahri, J. P. Draayer, and S. A. Moszkowski, Phys. Rev. Lett. **68**, 2133 (1992).
[17] A. L. Blokhin, C. Bahri, and J. P. Draayer, Phys. Rev. Lett. **74**, 4149 (1995).
[18] J. N. Ginocchio, Phys. Rev. Lett. **78**, 436 (1997).
[19] J. Meng, K. Sugawara-Tanabe, S. Yamaji, P. Ring, and A. Arima, Phys. Rev. **C 58**, R628 (1998).
[20] J. Meng, K. Sugawara-Tanabe, S. Yamaji, and A. Arima, Phys. Rev. **C 59**, 154 (1999).
[21] K. Sugawara-Tanabe, S. Yamaji, and A. Arima, Phys. Rev. **C 62**, 054307 (2000).
[22] P. Alberto, M. Fiolhais, M. Malheiro, A. Delfino, and M. Chiapparini, Phys. Rev. Lett. **86**, 5015 (2001).

[23] P. Alberto, M. Fiolhais, M. Malheiro, A. Delfino, and M. Chiapparini, Phys. Rev. **C 65**, 034307 (2002).
[24] R. Lisboa, M. Malheiro, P. Alberto, M. Fiolhais, and A. S. de Castro, Phys. Rev. **C 81**, 064324 (2010).
[25] S. Marcos, M. Lopez-Quelle, R. Niembro, L. N. Savushkin, and P. Bernardos, Phys. Lett. **B 513**, 30 (2001).
[26] S. Marcos, M. Lopez-Quelle, R. Niembro, L. N. Savushkin, Eur. Phys. J. **A 37**, 251 (2008).
[27] H. Z. Liang, P. W. Zhao, Y. Zhang, J. Meng, and N. V. Giai, Phys. Rev. **C 83**, 041301(R) (2011).
[28] J. N. Ginocchio, J. Phys. Conf. Ser. 267, 012037 (2011).
[29] A. Leviatan, Phys. Rev. Lett. **92**, 202501 (2004).
[30] S. Typel, Nucl. Phys. **A 806**, 156 (2008).
[31] A. Leviatan, Phys. Rev. Lett. **103**, 042502 (2009).
[32] H. Z. Liang, S. H. Shen, P. W. Zhao, J. Meng, Phys. Rev. **C 87**, 014334 (2013).
[33] J. Y. Guo, R. D. Wang, and X. Z. Fang, Phys. Rev. **C 72**, 054319 (2005).
[34] J. Y. Guo and X. Z. Fang, Phys. Rev. **C 74**, 024320 (2006).
[35] B. N. Lu, E. G. Zhao, and S. G. Zhou, Phys. Rev. Lett. **109**, 072501 (2012).
[36] J. Y. Guo, Phys. Rev. **C 85**, 021302(R) (2012)
[37] S. W. Chen and J. Y. Guo, Phys. Rev. **C 85**, 054312 (2012).
[38] S. G. Zhou, J. Meng, and P. Ring, Phys. Rev. Lett. **91**, 262501 (2003).
[39] C. Itzykson and J. B. Zuber, Quantum Field Theory (McGraw-Hill, New York, 1980).

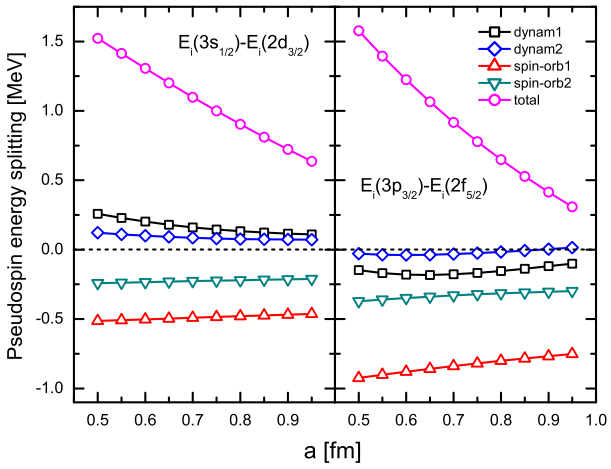

FIG. 1: (Color online) Comparisons of the contributions of the components relating the dynamical term and the spin-orbit interactions to the pseudospin energy splitting and their correlations with the surface diffuseness a for the $(3s_{1/2}, 2d_{3/2})$ and $(3p_{3/2}, 2f_{5/2})$ partners, where the "dynam1(spin-orb1)" and "dynam2 (spin-orb2)" correspond respectively to the $1/M^2$ order and the $1/M^3$ order perturbations for the dynamical components (the spin-orbit interactions). For guiding eyes, the total pseudospin energy splitting is plotted as "total".

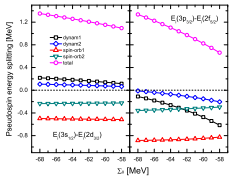

FIG. 2: (Color online) The same as Fig.1, but with the depth Σ_0 of the Woods-Saxon potential.

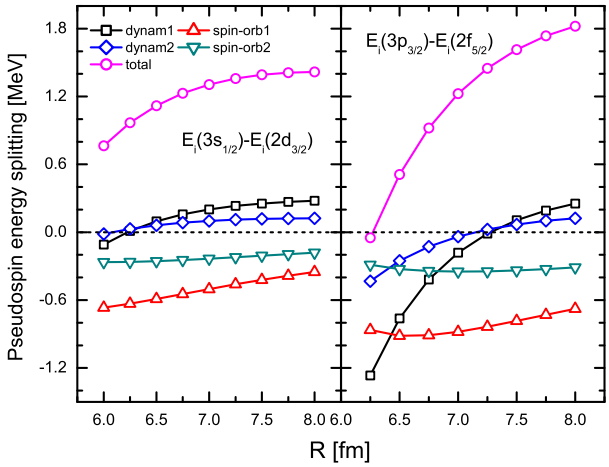

FIG. 3: (Color online) The same as Fig.1, but with the radius R of the Woods-Saxon potential.

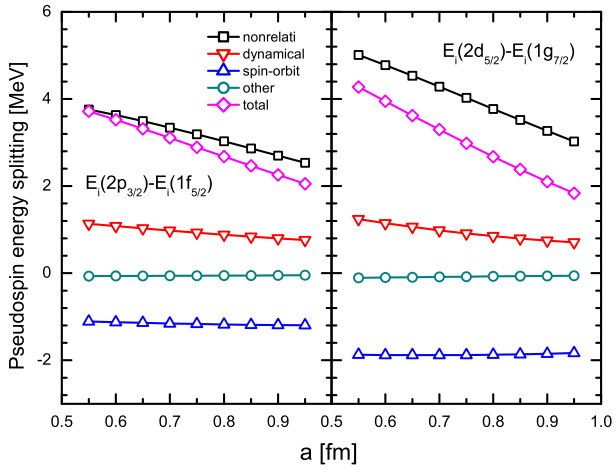

FIG. 4: (Color online) Comparisons of the contributions of all the terms in H_P to the pseudospin energy splitting and their correlations with the surface diffuseness a for the $(2p_{3/2}, 1f_{5/2})$ and $(2d_{5/2}, 1g_{7/2})$ partners, where "nonrelati" denotes the result in the nonrelativistic limit, "dynamical (spin-orbit)" denotes the data contributed by the dynamical term (the spin-orbit interactions), "other" marks a combination of the contributions of O_6, O_7, and O_8 to the pseudospin splitting, and "total" labels the total pseudospin energy splitting.

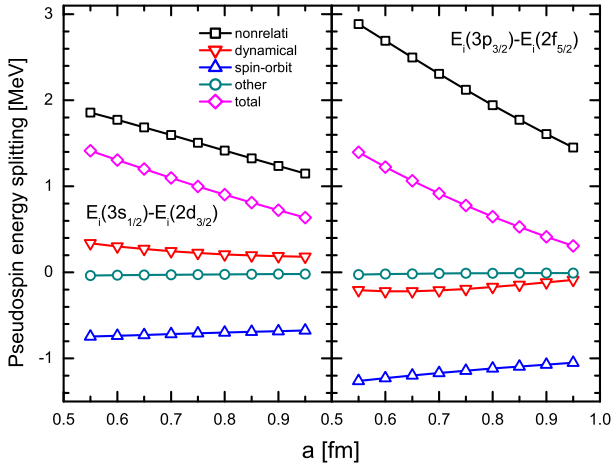

FIG. 5: (Color online) The same as Fig.4, but for the $(3s_{1/2}, 2d_{3/2})$ and $(3p_{3/2}, 2f_{5/2})$ partners.

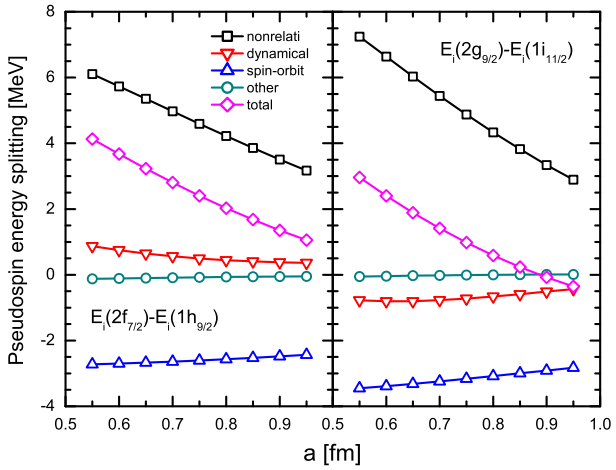

FIG. 6: (Color online) The same as Fig.4, but for the $(2f_{7/2}, 1h_{9/2})$ and $(2g_{9/2}, 1i_{11/2})$ partners.

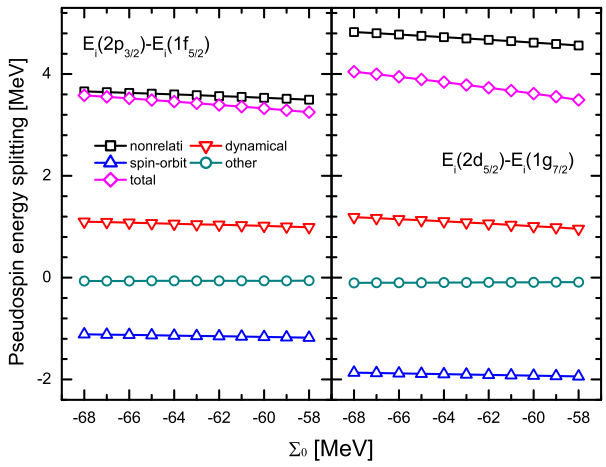

FIG. 7: (Color online) The same as Fig.4, but with the depth Σ_0 of the Woods-Saxon potential for the $(2p_{3/2}, 1f_{5/2})$ and $(2d_{5/2}, 1g_{7/2})$ partners.

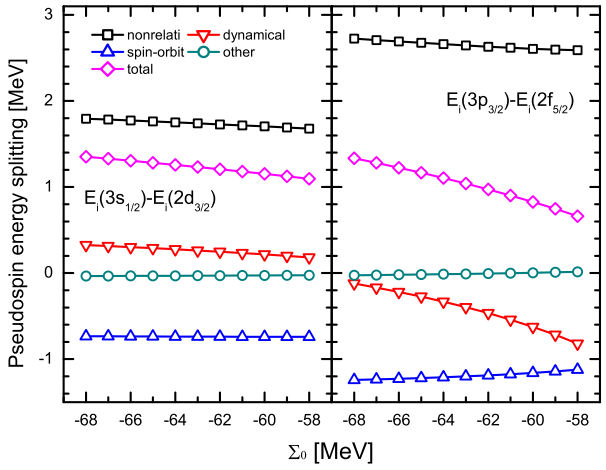

FIG. 8: (Color online) The same as Fig.7, but for the $(3s_{1/2}, 2d_{3/2})$ and $(3p_{3/2}, 2f_{5/2})$ partners.

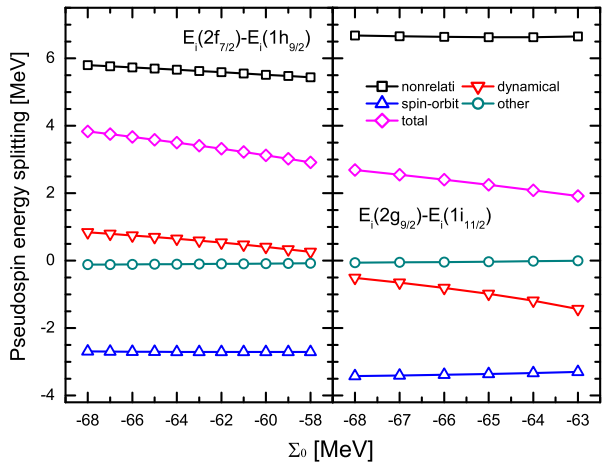

FIG. 9: (Color online) The same as Fig.7, but for the $(2f_{7/2}, 1h_{9/2})$ and $(2g_{9/2}, 1i_{11/2})$ partners.

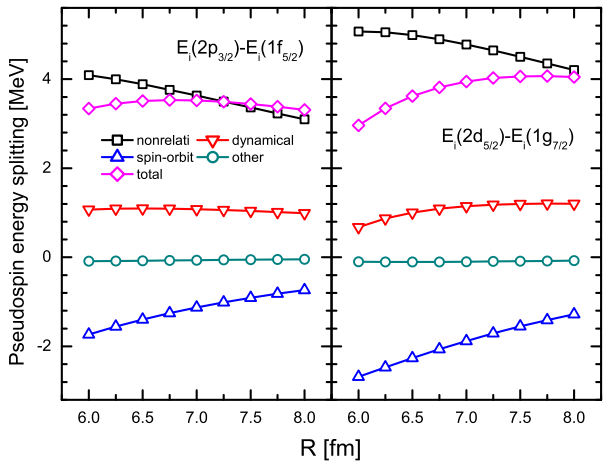

FIG. 10: (Color online) The same as Fig.4, but with the radius R of the Woods-Saxon potential for the $(2p_{3/2}, 1f_{5/2})$ and $(2d_{5/2}, 1g_{7/2})$ partners.

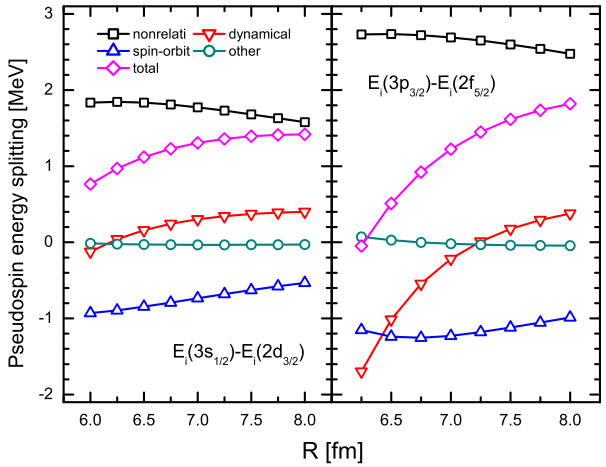

FIG. 11: (Color online) The same as Fig.10, but for the $(3s_{1/2}, 2d_{3/2})$ and $(3p_{3/2}, 2f_{5/2})$ partners.

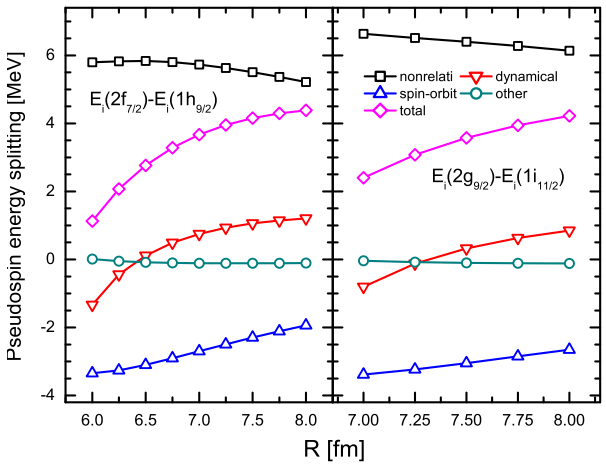

FIG. 12: (Color online) The same as Fig.10, but for the $(2f_{7/2}, 1h_{9/2})$ and $(2g_{9/2}, 1i_{11/2})$ partners.